Journal of Materials Processing Technology 213 (2013) 2145–2151

Contents lists available at ScienceDirect

Journal of Materials Processing Technology

journal homepage: www.elsevier.com/locate/jmatprotec

A parametric study of Inconel 625 wire laser deposition

T.E. Abioye, J. Folkes, A.T. Clare*

Manufacturing Division, Faculty of Engineering, University of Nottingham, NG7 2RD, United Kingdom

ARTICLE INFO

Article history:
Received 14 February 2013
Received in revised form 1 May 2013
Accepted 10 June 2013
Available online 20 June 2013

Keywords:
Laser
Deposition
Inconel 625
Wire
Dilution
Process characteristics

ABSTRACT

Laser deposition with wire offers saving potentials over powder based systems. These include a cleaner processing environment, reduced economic and environmental cost of producing the wire, better surface finish and higher material deposition rates. This technique is rapidly finding applications for the manufacture and repair of high value components. For the first time, the deposition of Inconel 625 wire for single tracks at varying processing parameters using a 2-kW Ytterbium doped fibre laser has been investigated. A process map predicting the process characteristics in terms of wire dripping, smooth wire transfer and wire stubbing at different cladding conditions has been developed. Track geometrical characteristics including aspect ratio and contact angle were evaluated using surface profilometry and optical microscopy. Scanning electron microscopy equipped with energy dispersive X-ray spectroscopy was used to determine the dilution ratio (%) of the tracks. Wire deposition volume per unit length of track and energy per unit length of track were found to be key parameters influencing both the process and track geometrical characteristics. Aspect ratio and dilution ratio showed positive dependency whereas contact angle showed negative dependency on energy per unit length of track. Conversely, material deposition volume per unit length of track varied directly with contact angle but inversely with aspect ratio and dilution ratio (ranging from 0% to 24%). Processing conditions at which a combination of favourable single track properties including low contact angle (<80°), minimal dilution ratio (5–13%) and high surface quality were achieved are presented. These properties are required for depositing overlapped tracks of good surface finish, minimal dilution and free of inter-run porosity.

1. Introduction

Laser cladding had been shown to be an effective metal surface coating technique capable of increasing component lifetime

These include strong metallurgical bond at the clad–substrate interface (Chen et al., 1996), minimal distortion of the substrate (Desale et al., 2009), low dilution (Huang, 2011), minimal porosity (Sexton et al., 2002) and controllable heat input often producing a small heat affected zone (HAZ) (Huang et al., 2004).

Laser cladding involves the use of a high-precision heat source to create a melt pool by simultaneously melting the additive material and a thin layer of a substrate. The relative movement of the laser beam and the substrate forms a track. The track is most often referred to as a clad bead. Additive material which is either in powder or wire form can be delivered using three methods. Preplacing powder in the form of slurry on the substrate prior to heat application is less flexible compared with other methods. The coaxial powder form.

Extensive research in laser cladding using metal powder has been undertaken for enhanced surface performance. Consequently, a range of high corrosion and wear resistant materials had been processed in this way. Desale et al. (2009) researched on the erosion wear behaviour of Colmonoy-6 and Inconel 625 powders. Baldridge et al. (2013) have reported the analysis of laser cladding of Inconel 690 powder on Inconel 600 for corrosion protection in nuclear applications. Cobalt-based alloys have also been the subject of some investigation by Lusquiños et al. (2009). Quantitative characterisation of porosity in stainless steels LENS powders and deposits have also been reported by Susan et al. (2006). Common observations amongst these processes are high surface roughness, low powder deposition rate and susceptibility of the clad to porosity usually caused by the entrapment of gas in the powder. As a result, cladding with powder material is less economical for coating large areas, especially, where high dimensional accuracy

* Corresponding author. Tel.: +44 0115 951 4109; fax: +44 0115 951 3800.
E-mail address: adam.clare@nottingham.ac.uk (A.T. Clare).

0924-0136
http://dx.doi.org/10.1016/j.jmatprotec.2013.06.007

Table 1
Chemical compositions of Inconel 625 wire and 304 stainless steel in wt.%.

Element	Ni	Cr	Mn	Si	Al	Ti	Fe	C	Mo	Nb	P	S
Inconel 625	Bal	22.46			0.26	0.26	0.14	0.02	8.84	3.46		
304 stainless steel	7.86	18.58	1.78	0.42			Bal	0.08			0.10	0.03

is of paramount importance. Also, presence of porosity is disadvantageous to the corrosion behaviour of the clad (Zareie Rajani et al., 2013).

Due to its combination of favourable properties such as high temperature strength, excellent corrosion resistance, high ductility and good stress corrosion cracking resistance, Inconel 625 (a nickel based superalloy) has been the material choice for a diverse range of applications. These include gas turbine ducting, furnace hardware and components exposed to seawater (Paul et al., 2007). More importantly, the low dilution of the laser cladding technique coupled with the excellent corrosion properties of the alloy had extended the applications of Inconel 625 laser coating to oil and gas industry. Down-hole drilling equipment are manufactured from stainless steels because of their high impact strength, reasonable corrosion resistance and low cost (Sue et al., 2010). The resistance offered by the steels against corrosion is limited because steels suffer localised corrosion in specific environments, particularly in chloride ion rich solutions (Mahmood et al., 2012). Following this fact, the lifetime performance of off-shore equipment in harsh corrosive environment is currently being increased by laser coating the surface of the steels with Inconel 625 alloy. To date, a number of studies have been reported on laser deposition of Inconel 625 powder, for example, the microstructural evolution (Dinda et al., 2009), optimising processing parameters (Paul et al., 2007), thin wall manufacture (Gao et al., 2011) and corrosion properties of coatings (Tuominen et al., 2003). However, laser deposition using Inconel 625 wire as a feedstock material rather than powder has not been undertaken.

Laser cladding with lateral wire feeding system, compared with powder based feeding systems, offers better rewards such as increased material usage efficiency (Syed et al., 2005), improved surface quality of the deposit (Heralic, 2009), lower cost of preparing the wire materials (Kim and Peng, 2000) and higher material deposition rates (Syed et al., 2005). However, wire based systems are highly sensitive to changes in processing condition. As a result, it is important to establish a balance of several impacting processing parameters such as wire tip position in the meltpool, feed angle, feed direction, laser spot size, laser power (P), wire feed rate (WFR) and traverse speed (V) before a stable wire deposition process can be achieved.

Three wire tip positions, i.e. the centre, leading and trailing edges, in the meltpool have been identified by Syed and Li (2005). When the wire tip was positioned at the trailing edge, Syed and Li (2005) discovered that the deposition process was mainly characterised by droplet transfer of wire (dripping) forming irregular beads whereas smooth wire transfer was only found possible at the centre and leading edge of the meltpool. Mok et al. (2008) established that wire feed angle around 45° gives the highest track deposition efficiency during diode laser cladding of Ti–6Al–4V wire with front feeding orientation. In the past, optimisation of the processing parameters for Nd–YAG laser deposition with wire of ZE41A-T5, a magnesium alloy, using Taguchi method for parameter design had been undertaken (Cao et al., 2008). The results include the variation of dilution ratio with the main processing parameters. However, a study of the laser deposition with wire process characteristics at varying processing parameters is absent from the literature. Also, significantly few authors have reported on the investigation of the wetting angle usually referred to as contact angle of laser deposited wire tracks at varying cladding conditions.

In this study, single tracks of Inconel 625 wire were deposited at varying processing parameters via laser cladding. The primary objectives are of two folds. Firstly, a process map which predicts Inconel 625 wire fibre laser deposition process characteristics at varying processing parameters will be developed. Secondly, processing parameters at which a combination of favourable single track properties including low contact angle (<80°), minimal dilution ratio (5–13%) and high surface quality can be achieved will be determined. These properties are quality criteria for depositing overlapped tracks of good surface finish, minimal dilution and free of inter-run porosity.

2. Experimental

2.1. Materials

Plates of dimension 100 mm × 180 mm × 6 mm were machined from austenitic stainless steel AISI 304 and used as substrate material. These were grit blasted and cleaned with acetone before the deposition runs so as to improve substrate surface laser absorptivity and remove contaminants, respectively. The additive material is Inconel 625 wire of 1.2 mm diameter supplied by VBC group, Loughborough, UK. Table 1 gives the chemical compositions of Inconel 625 wire and AISI 304 stainless steel, as quoted by the manufacturers.

2.2. Laser processing

A diagram of the laser deposition system used in this study is shown in Fig. 1. Deposition was performed using a 2 kW Ytterbium doped fibre laser (IPG Photonics) operating at 1070 nm wavelength. The beam was focused to a small round spot of approximately 3.1 mm at 20 mm away from focus giving a 212 mm working distance with a Gaussian energy distribution. Inconel 625 wire was "front fed" at an angle of 42 ± 1° to the horizontal so as to aim the wire tip at the centre of the meltpool. A WF200DC wire feeder (Redman Controls and Electronic Ltd.) was used.

Single tracks were deposited, at varying processing parameters, on the steel plates inside a transparent enclosure (bag) which was evacuated and back-filled with high purity argon gas supplied at 0.42 l s^{-1}. The utilised processing parameters were selected following preliminary trials so as to reduce the number

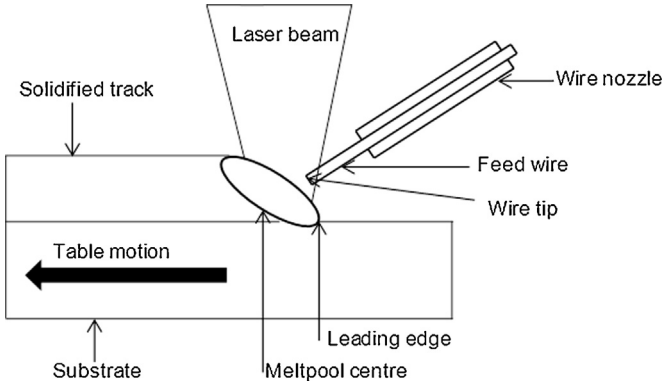

Fig. 1. Schematic representation of the laser deposition system.

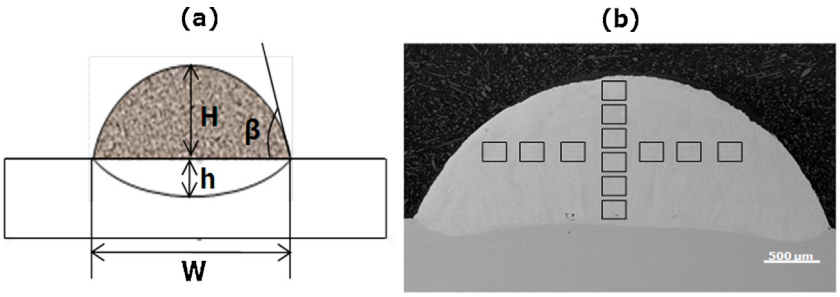

Fig. 2. Track characterisation (a) track metrics (b) SEM micrograph of a transversely sectioned sample.

of experimental runs required. Real-time observation of the deposition runs was recorded by a camera attached to precitec YW50 laser head. Table 2 gives the details of the processing parameters used for the tracks deposition.Tracks were deposited with combinations of laser power and traverse speeds with varying wire feed rates ranging from 6.7 mm s^{-1} until stubbing was observed (i.e. the wire tip colliding with the substrate). This process was repeated for all possible combinations of processing parameters within the selected fixed range of laser power and traverse speed (totalling 125 tracks). Two tracks were deposited at each cladding condition to provide a degree of verification.

2.3. Track characterisation

Fig. 2a shows a schematic diagram of typical track geometry. The tracks heights and widths were measured at three different points along their lengths using a Taylor Hobson surface profiler (Talysurf CLI 1000). For the purpose of microstructural investigation, track samples were transversely sectioned, mounted in conducting resin and sequentially ground and polished to a 1 μm surface finish. Then, the track samples were electrolytically etched using 70% orthophosphuric acid in water (typically 6 V for 3 s). The tracks microstructures were examined under scanning electron microscopy (SEM) using a back scattered electron (BSE) signal. Quantitative energy dispersive X-ray analysis (EDXA) was utilised in determining the elemental composition of Fe in the tracks by conducting area scan (200 μm × 200 μm) analysis along and across the height of each cross-sectioned track, as shown in Fig. 2b.

2.4. Definition of terms

Energy per unit length of track (E_L) in J mm^{-1} is a combined effect of laser power (P) in Watts and traverse speed (V) in mm s^{-1}, and it is defined by Eq. (1). The deposition volume per unit length of track pass (D_{VL}) in mm^3 mm^{-1} has the traverse speed and wire feed rate (WFR) in mm s^{-1} as the determining variables. The constant 'A' in Eq. (2) is the cross-sectional area of the wire in mm^2.

$$E_L = \frac{P}{V} \tag{1}$$

Table 2
Processing parameters.

Parameters	Value	Unit
Laser power	1.0–1.8	kW
Wire feed rate	6.7–23.3	mm s^{-1}
Traverse speed	1.7–8.5	mm s^{-1}
Separation distance between two consecutive tracks	10	mm
Argon gas flow rate	0.42	l s^{-1}
Wire diameter	1.2	mm
Wire feeding angle	42 ± 1	degrees

$$D_{VL} = \frac{A \times WFR}{V} \tag{2}$$

$$\beta = 2\arctan\left(\frac{2H}{W}\right) \tag{3}$$

$$\eta = \frac{\rho_c(X_{c+s} - X_c)}{\rho_s(X_s - X_{c+s}) + \rho_c(X_{c+s} - X_c)} \tag{4}$$

The contact angle (β) was calculated from the values of the track height (H) and width (W) using Eq. (3) (de Oliveira et al., 2005) while the dilution ratio (η) was determined from the composition of the track using Eq. (4) (Toyserkani et al., 2005). ρ_c and ρ_s in Eq. (4) are the densities of the feed material (Inconel 625 wire; 8.44×10^{-3} g mm^{-3}) and substrate (AISI 304 stainless steel; 8.04×10^{-3} g mm^{-3}), respectively. X_{c+s} and X_s are the mean weight percent of Fe in total surface of track region and substrate, respectively while X_c is the weight percent of Fe in the additive material.

3. Results and discussion

3.1. Wire deposition characteristics

As the wire feed rate was sequentially varied for each combination of laser power and traverse speed, entirely different deposition process characteristics were observed. The observed characteristics were wire dripping, smooth wire transfer and wire stubbing. These are typical of wire laser deposition process. However, each material system behaved differently at every condition of laser deposition process. Inconel 625 coatings on oil and gas pipelines is being increasingly utilised because of its excellent protection against corrosion (Xu et al., 2013). As a result, optimising Inconel 625 wire laser deposition process to producing continuous track with acceptable dimension is essential to its application in this industry. A process map valid for the fibre laser deposition of Inconel 625 wire of Ø1.2 mm for laser power range of 1.0–1.8 kW, traverse speed ranging from 1.7 to 5.0 mm s^{-1} and wire feed rate 6.7–23.3 mm s^{-1} was developed. As shown in Fig. 3, five different regions were clearly defined in the map with 1–5 representing dripping, dripping may occur, smooth wire flow, stubbing may occur and stubbing regions, respectively. Each processing condition was represented by a point on the map. The combined parameter on the y-axis of the map was found by dividing laser power by the traverse speed (see Eq. (1)). Wire deposition volume per unit length on the x-axis is a function of wire feed rate, traverse speed and cross-sectional area of the feed wire at a given processing condition (see Eq. (2)).

Fig. 4 presents the typical examples of tracks deposited by deposition process characterised with dripping of wire (droplet transfer), smooth transfer of wire (smooth deposition) and stubbing of wire. The ideal scenario (i.e. cladding conditions that produce track of high surface quality and acceptable dimensions) is found when there is smooth transfer of wire into the meltpool. This was observed whenever the wire tip melted at the point or close to the

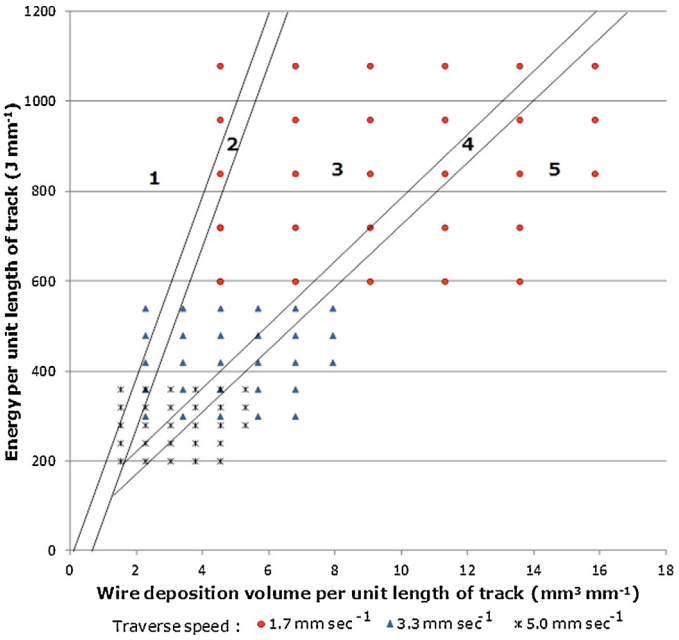

Fig. 3. A process map for Inconel 625 wire laser deposited tracks.

point of intersection with the meltpool. The processing conditions that produced smooth transfer of wire are contained in the region 3 of the process map.

When the wire feed rate was excessively low for a fixed combination of traverse speed and laser power, intermittent dripping of wire was observed. This produced discontinuous tracks as shown in Fig. 4. At a very low wire feed rate, the wire tip interacted too long with the laser beam such that it absorbed heat energy sufficient for its melting. As a result, the wire tip melted before intersecting with the meltpool. This produced intermittent dripping of molten wire as the substrate traversed. Similar effect was observed whenever the energy per unit length of track was excessive for a fixed wire deposition volume per unit length of track.

At a cladding condition when the wire feed rate was excessively high for a fixed combination of traverse speed and laser power, the feed wire interacted briefly with the laser beam. As result, the wire entered the meltpool in a nearly solid form resulting in the collision of the wire tip with the solid substrate at the base of the meltpool. A collision with the substrate caused the wire tip to move away from the centre of the meltpool. In the process, the wire was eventually melted by the energy in the meltpool and solidified as tracks with an irregular shape. At an extremely high wire feed rate, the wire remained unmelted. This was due to the fact that wire deposition volume per unit length of track was too high for the given energy per unit length of track.

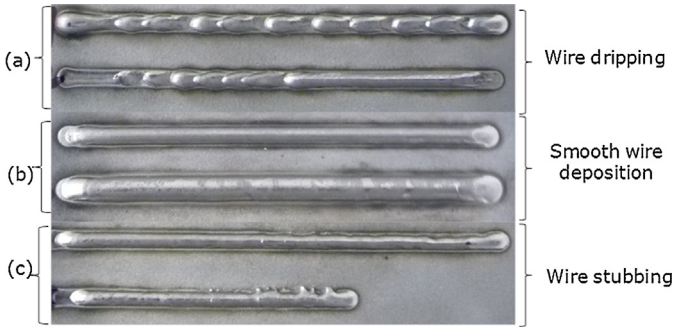

Fig. 4. Typical deposits of Inconel 625 wire.

It can be observed from the map that region 1 (i.e. wire dripping region) widens whereas region 5 (wire stubbing region) becomes narrower with increasing energy per unit length of track. This confirms the fact that increased energy produced higher heat input, hence, quicker melting of the feed wire before its intersection of the meltpool. Therefore, more dripping and less stubbing of wire were observed.

Also, as the wire deposition volume per unit length of track increased in the process map, the deposition process characteristics transited from wire dripping to smooth wire deposition and then wire stubbing. This shows that the wire dripping can be eliminated, as expected, by either reducing the energy per unit length of track or increasing the wire deposition volume per unit length of track. Also, wire stubbing can be reversed to ideal scenario by either increasing the energy per unit length of track or decreasing the wire deposition volume per unit length of the track.

Region 2 (i.e. wire dripping may occur region) formed the boundary between the dripping region and smooth wire deposition region. Laser deposition processes performed at the conditions corresponding to this region produced inconsistent characteristics because each of these processes were characterised with dripping and smooth wire transfer effects after at least two trials. As a result, it was difficult to correctly classify them either into dripping or smooth deposition region.

Region 4 is the boundary between the smooth deposition region and the wire stubbing region. Due to inconsistence in their process characteristics, cladding conditions that gave deposition run of both wire stubbing and smooth wire transfer after at least two different trials were grouped in this region. Finally, the map predicts that smooth wire transfer may not be practicable, with this arrangement, when cladding below energy per unit length of track of 200 J mm^{-1}.

3.2. Clad characteristics

3.2.1. Width–height aspect ratio

The width–height (*W*–*H*) aspect ratio was calculated from the results obtained from the height and width measurements of the tracks. Since, past works have clearly indicated that track aspect ratio is significant to depositing inter-run porosity free overlapped tracks (Pinkerton and Li, 2008), aspect ratio of single track deposits can therefore be used as a quality criterion for the deposition of overlapped tracks.

Fig. 5 shows that the track aspect ratio increases with increasing the traverse speed and laser power but with decreasing the wire feed rate, provided, other factors remain constant. Similar results were found for fibre laser micro-cladding of Co-based alloys on AISI 304 stainless steel (Lusquiños et al., 2009). The response of the aspect ratio can be explained by the wire volume deposited per unit length of track. Decreasing the wire feed rate and/or increasing the traverse speed reduced the wire deposited volume per unit length of track. This resulted in track of reduced height. However, the track width was invariant with the wire deposition volume (mm^3 mm^{-1}). These effects produced decreased aspect ratio. Higher aspect ratio obtained at higher power is due to pronounced flattening effect (increase in width) of laser power on the track geometry. Since width is the numerator in the ratio therefore any change that increases it and/or decreases H (denominator) will increase the value of the ratio.

3.2.2. Dilution ratio

Generally, dilution is the percentage of the total volume of the substrate material in the track contributed by melting of the substrate. Though it is undesirable in cladding processes, some minimum (about 3–8%) (Qian et al., 1997) is required before a fully dense bond is achievable in a track.

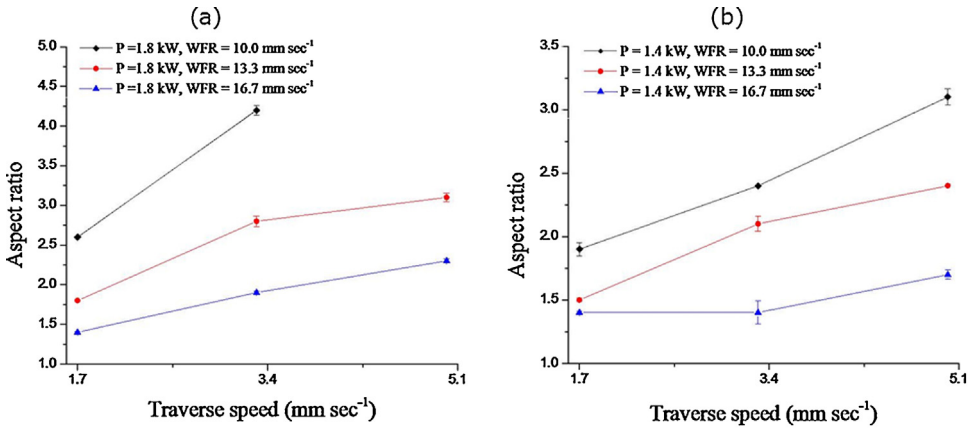

Fig. 5. Variation of track aspect ratio as a function of the main processing parameters (a) $P = 1.8$ kW and (b) $P = 1.4$ kW.

Dilution ratio analysis was carried out from the composition of the tracks as described in Section 2.4. As shown in Fig. 6, elemental composition analysis (i.e. EDXA) established that Fe content, hence, the percentage dilution of the examined track samples increased with increasing laser power and traverse speed but with decreasing wire feed rate. As the laser power was increased, a higher volume of the substrate was melted due to increased energy input. Also, there was sufficient mixing and vigorous meltpool movement. This caused an increased percentage of the molten substrate (mainly Fe) mixing with the track layer thus producing higher dilution ratio.

At increased wire feed rate, more wire volume (due to increased deposition rate) was deposited into the meltpool producing bigger track. Also, there was increased laser energy interruption by the feed wire causing significant reduction in the fraction of energy reaching the substrate. As a result, low melted depth into the substrate was observed. Also, the viscosity of the meltpool is believed to be higher at higher WFR therefore reducing the vigour, hence, mixing in the meltpool. Eventually, there was reduced dilution of Fe from the substrate.

When the traverse speed was increased, two things became apparent. Firstly, the deposited wire volume per unit length of track reduced, producing smaller track. Secondly, the energy per unit length of track also decreased causing reduced melted depth into the substrate. However, as shown in Fig. 7, the change in melted depth into the substrate is relatively insignificant compared with the change in the track volume. As a result, increase in dilution ratio was observed in the track as the speed increased.

3.2.3. Contact angle

As shown in Fig. 6, contact angle was found to increase with increasing wire feed rate but decreased with increasing traverse speed and laser power. The results show that apart from the surface tension, processing parameters also influence the wetting (i.e. contact angle) of laser deposited tracks. Fig. 8 clearly revealed that an increase in wire feed rate and/or decrease in traverse speed

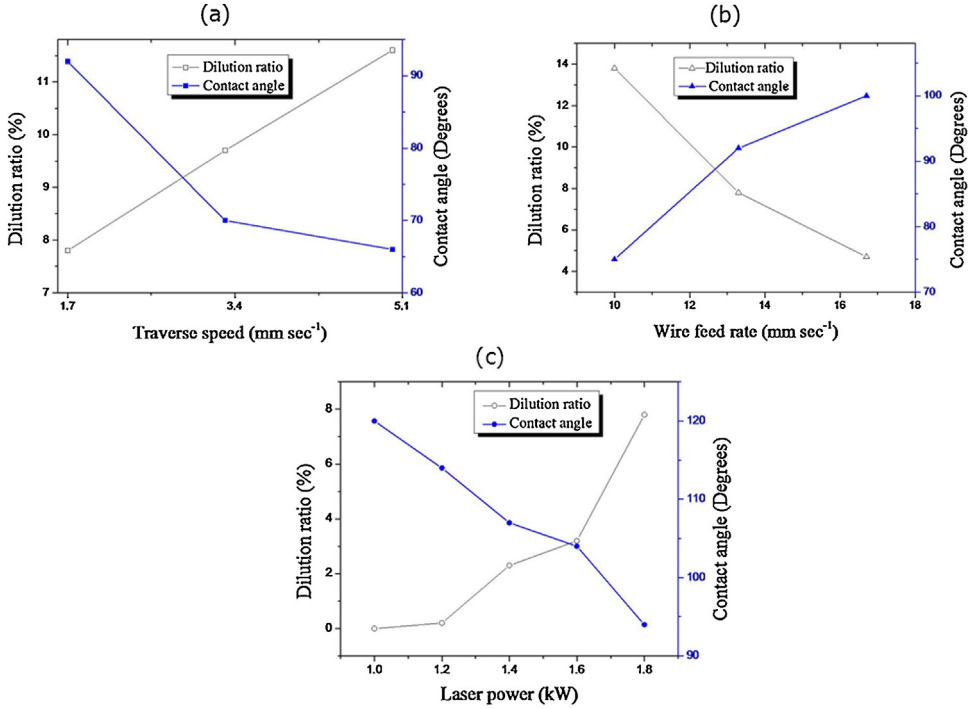

Fig. 6. Variation of dilution ratio and contact angle with the main processing parameters. (a) $P = 1.8$ kW, WFR = 13.3 mm s^{-1}, (b) $P = 1.8$ kW, $V = 1.7$ mm s^{-1} and (c) $V = 1.7$ mm s^{-1}, WFR = 13.3 mm s^{-1}.

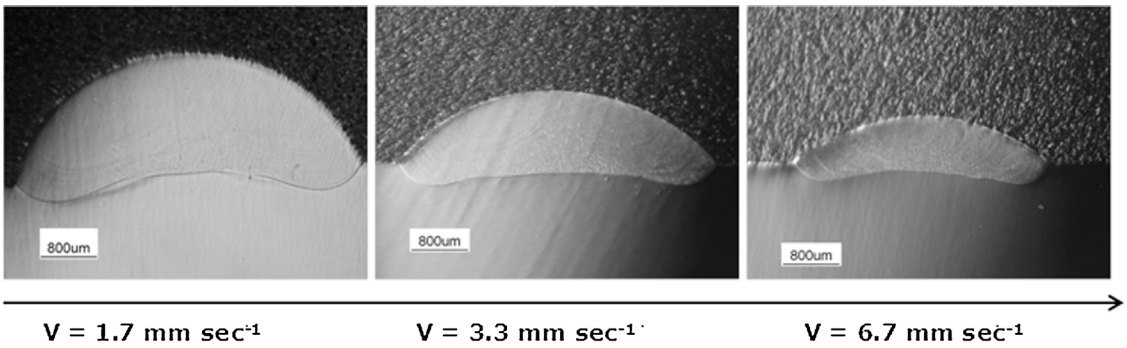

Fig. 7. Etched optical macro-photographs of laser track cross-sections for Inconel 625 wire at laser power of 1800 W and wire feed rate of 10 mm s^{-1}.

(i.e. increasing the wire deposited volume per unit length of track) resulted in tracks becoming more spherical. At a low wire deposition volume per unit length of track, a parabolic shaped track of contact angle lower than 90° was formed. However, as the wire feed rate increased or traverse speed decreased, more wire was deposited per unit length of track until it was sufficient to form a track strip with a more spherical shape in cross-section. Further increases to wire deposition volume resulted in swollen flanks of the track thus producing track with an obtuse contact angle.

High energy per unit length of track resulting from increased laser power produced hotter meltpool. The high energy meltpool expedited the melting of the wire, increased the fluidity and vigour of the meltpool. This caused the molten pool to spread, instead of building height, away from its centre. As a result, the solid substrate at meltpool boundary melted and the meltpool size increased. Eventually, wider tracks with low contact angles were formed.

3.2.4. Overlapping tracks

Geometrical characterisation of all the deposited tracks revealed that there is a sharp contrast in the growth trends of contact angle and dilution ratio with the processing parameters.

The concern was to determine suitable processing condition(s) that give good surface quality tracks with low contact angle (<80°) and minimal dilution ratio (ranging between 5% and 13%). The combination of these single track properties is important for the deposition of overlapped tracks of high surface quality, minimal dilution and no inter-run porosity. Fe diffusion from the substrate into the track has a deteriorating effect on the corrosion behaviour of the superalloy (Zareie Rajani et al., 2013). As a result, a minimum dilution ratio between 3% and 8% had been established to be appropriate for obtaining a fully dense track-substrate bond. Values outside this range were considered undesirable. In this study, processing conditions that produced single tracks with 5–13% dilution ratio were selected for depositing overlapped tracks because it

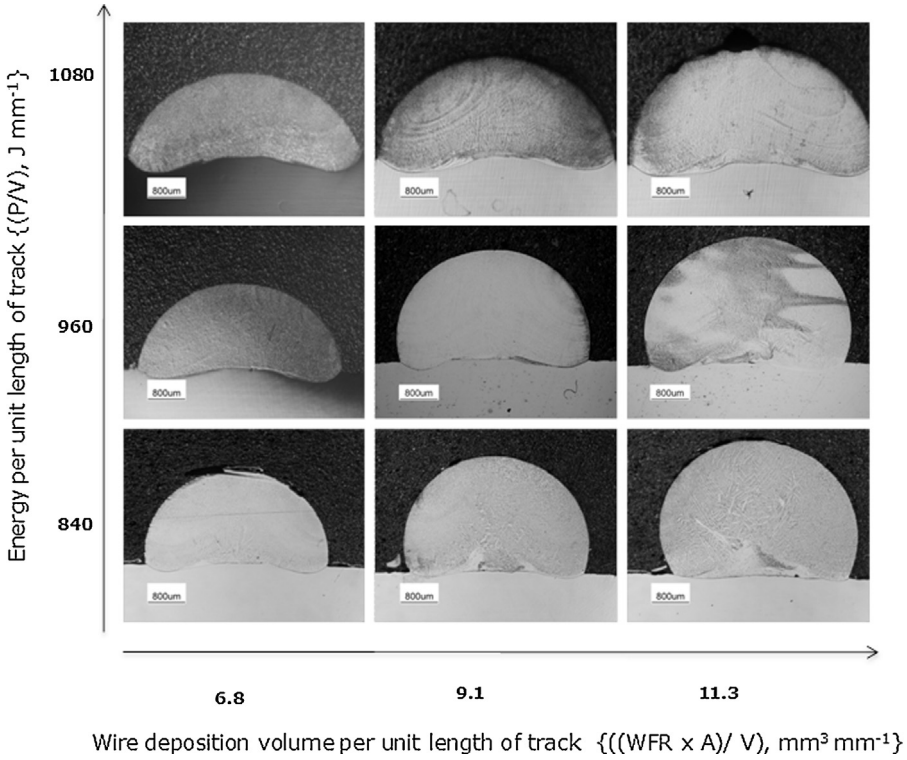

Fig. 8. Etched optical macro-photographs of laser track cross-sections for Inconel 625 wire at traverse speed of 1.7 mm s^{-1}.

Table 3
Processing conditions at which a combination of favourable single track properties including low contact angle (<80°), minimal dilution ratio (5–13%) and high surface quality were achieved.

S/N	Laser power (kW)	Traverse speed (mm s^{-1})	Wire feed rate (mm s^{-1})	Process characteristics	Dilution (%)	Contact angle (degrees)	Aspect ratio
1	1.8	1.7	10.0	Smooth wire deposition	11.9	75	2.6
2	1.8	3.3	13.3	Smooth wire deposition	10.1	70	2.8
3	1.8	5.0	13.3	Smooth wire deposition	11.0	66	3.1
4	1.6	3.3	10.0	Smooth wire deposition	11.6	67	3.0
5	1.6	5.0	13.3	Smooth wire deposition	6.4	76	2.6
6	1.4	5.0	10.0	Smooth wire deposition	8.0	76	2.5
7	1.2	3.3	6.7	Smooth wire deposition	5.4	73	2.7

was predicted that reduced dilution ratio is obtainable in the overlapped layers. This is due in part to the additional heating of the adjacent tracks. The processing conditions at which the combination of favourable single track properties was found are presented in Table 3.

Excessively low energy per unit length of track caused majority of the depositions performed at 1.0 kW laser power to be characterised by wire stubbing. Processing parameters where smooth deposition was observed, the desirable combination of contact angle and dilution ratio was not achieved.

4. Conclusion

In this work, a process map for the fibre laser deposition of Inconel 625 wire predicting the process characteristics at varying processing parameters has been developed. Energy per unit length of track and wire deposition volume per unit length of track significantly influence both the deposition process characteristics and the track geometrical characteristics. Excessively low and high wire deposition volume per unit of track for a given energy per unit length of track resulted in wire dripping and wire stubbing, respectively. Tracks of high surface quality and acceptable dimension were deposited whenever there was smooth transfer of wire. At energy per unit length of track below 200 J mm^{-1}, it is impracticable, for the set up employed in this study, to successfully deposit Inconel 625 wire track of good surface quality and acceptable dimension.

The individual effects of laser power, traverse speed and wire feed rate on the track characteristics were investigated and the following conclusions were drawn.

- It was found that the contact angle increases whereas dilution ratio and aspect ratio decreases with increasing wire feed rate.
- Both the dilution ratio and aspect ratio show positive whereas contact angle shows negative dependency on the traverse speed.
- Dilution ratio and aspect ratio varied directly but contact angle varied inversely with the laser power.

Finally, processing conditions at which a combination of favourable single track properties including low contact angle (<80°), dilution ratio ranging between 5% and 13% and high surface quality can be achieved are presented.

The future work includes the microstructural characterisation of the single tracks as well as the characterisation and corrosion study of the overlapped tracks deposited at the determined conditions presented in this study.

Acknowledgements

The authors would like to thank Petroleum Technology Development Fund, Nigeria for sponsoring this research. The authors also acknowledge the expertise and technical input from Mr. Stuart Branston.

References

Baldridge, T., Poling, G., Foroozmehr, E., Kovacevic, R., Metz, T., Kadekar, V., Gupta, M.C., 2013. Laser cladding of Inconel 690 on Inconel 600 superalloy for corrosion protection in nuclear applications. Optics and Lasers in Engineering 51, 180–184.
Cao, X., Xiao, M., Jahazi, M., Fournier, J., Alain, M., 2008. Optimization of processing parameters during laser cladding of ZE41A-T5 magnesium alloy castings using Taguchi method. Materials and Manufacturing Processes 23, 413–418.
Chen, Z., Lim, L.C., Qian, M., 1996. Laser cladding of WC–Ni composite. Journal of Materials Processing Technology 62, 321–323.
de Oliveira, U., Ocelík, V., De Hosson, J.T.M., 2005. Analysis of coaxial laser cladding processing conditions. Surface and Coatings Technology 197, 127–136.
Desale, G.R., Paul, C.P., Gandhi, B.K., Jain, S.C., 2009. Erosion wear behavior of laser clad surfaces of low carbon austenitic steel. Wear 266, 975–987.
Dinda, G.P., Dasgupta, A.K., Mazumder, J., 2009. Laser aided direct metal deposition of Inconel 625 superalloy: microstructural evolution and thermal stability. Materials Science and Engineering A 509, 98–104.
Gao, S., Zhou, Y., Xi, M., 2011. Investigation on Inconel 625 Alloy Thin-Walled Parts by Direct Laser Fabrication, Advanced Material Research. Trans Tech Publications, Switzerland, pp. 3687–3691.
Heralic, A., 2009. Towards full Automation of Robotized laser Metal-Wire Deposition, Department of Signals and Systems. CHALMERS University of Technology, Goteborg, Goteborg, Sweden.
Huang, S.W., Samandi, M., Brandt, M., 2004. Abrasive wear performance and microstructure of laser clad WC/Ni layers. Wear 256, 1095–1105.
Huang, Y., 2011. Characterization of dilution action in laser-induction hybrid cladding. Optics and Laser Technology 43, 965–973.
Kim, J.-D., Peng, Y., 2000. Plunging method for Nd: YAG laser cladding with wire feeding. Optics and Lasers in Engineering 33, 299–309.
Lusquiños, F., Comesaña, R., Riveiro, A., Quintero, F., Pou, J., 2009. Fibre laser micro-cladding of Co-based alloys on stainless steel. Surface and Coatings Technology 203, 1933–1940.
Mahmood, K., Stevens, N., Pinkerton, A.J., 2012. Laser clad corrosion protection for mild and harsh environments. Journal of Surface Engineering.
Mok, S.H., Bi, G., Folkes, J., Pashby, I., 2008. Deposition of Ti-6Al-4V using a high power diode laser and wire, Part I: Investigation on the process characteristics. Surface and Coatings Technology 202, 3933–3939.
Paul, C.P., Ganesh, P., Mishra, S.K., Bhargava, P., Negi, J., Nath, A.K., 2007. Investigating laser rapid manufacturing for Inconel-625 components. Optics and Laser Technology 39, 800–805.
Pinkerton, A.J., Wang, W., Li, L., 2008. Component repair using laser direct metal deposition. Journal of Engineering Manufacture 222, 827–836.
Qian, M., Lim, L.C., Chen, Z.D., Chen, W.I., 1997. Parametric studies of laser cladding processes. Journal of Materials Processing Technology 63, 590–593.
Sexton, L., Lavin, S., Byrne, G., Kennedy, A., 2002. Laser cladding of aerospace materials. Journal of Materials Processing Technology 122, 63–68.
Sue, S.H., Qiu, B.H., et al., 2010. Improving hardfacing for drill bits and drilling tools. Journal of Thermal Spray Technology.
Susan, D.F., Puskar, J.D., Brooks, J.A., Robino, C.V., 2006. Quantitative characterization of porosity in stainless steel LENS powders and deposits. Materials Characterization 57, 36–43.
Syed, W.U.H., Li, L., 2005. Effects of wire feeding direction and location in multiple layer diode laser direct metal deposition. Applied Surface Science 248, 518–524.
Syed, W.U.H., Pinkerton, A.J., Li, L., 2005. A comparative study of wire feeding and powder feeding in direct diode laser deposition for rapid prototyping. Applied Surface Science 247, 268–276.
Toyserkani, E., Khajepour, A., Corbin, S., 2005. Laser Cladding. CRC Press.
Tuominen, J., Vouristo, P., Mantyla, T., Latokartano, J., Vihinen, J., Andersson, P.H., 2003. Microstructure and corrosion behaviour of high power diode laser deposited Inconel 625 coatings. Journal of Laser Applications, 15.
Xu, L.Y., Li, M., Jing, H.Y., Han, Y.D., 2013. Electrochemical behavior of corrosion resistance of X65/Inconel 625 welded joints. International Journal of Electrochemical Science 8, 2069–2079.
Zareie Rajani, H.R., Akbari Mousavi, S.A.A., Madani Sani, F., 2013. Comparison of corrosion behavior between fusion cladded and explosive cladded Inconel 625/plain carbon steel bimetal plates. Materials and Design 43, 467–474.